Journal of the Serbian Chemical Society
JSCS-info@shd.org.rs • www.shd.org.rs/JSCS
J. Serb. Chem. Soc. *87* (12) 1395–1407 (2022)
JSCS–5602
Original scientific paper
Published 18 November 2022

Ammonia removal by natural and modified clinoptilolite

AYTAÇ GÜNAL[1] and BURCU ERDOĞAN[2]*

[1]*Eskisehir Technical University, Graduate School of Sciences, Yunusemre Campus, 26470 Tepebasi, Eskisehir, Turkey and* [2]*Eskisehir Technical University, Faculty of Science, Department of Physics, Yunusemre Campus, 26470 Tepebasi, Eskisehir, Turkey*

(Received 10 November 2021, revised 30 May, accepted 11 June 2022)

Abstract: In this study, cation exchange and acid activation processes were applied to determine the effects of different cationic compositions of clinoptilolite on ammonia adsorption properties. Thermogravimetric (TG), differential thermal analysis (DTA), X-ray diffraction (XRD), X-ray fluorescence (XRF) and nitrogen adsorption techniques were used for the characterization of the clinoptilolite samples. As a result of ion exchange and acid activation, the amount, type and location of exchangeable cations in the structure significantly affected the thermal properties, as well as NH_3 removal efficiency. Ammonia adsorption isotherms were obtained at 298 K up to 100 kPa volumetrically. In addition, NH_3 adsorption capacities of the clinoptilolite samples within this study (3.823 to 5.372 mmol g^{-1}) were compared with those of the other materials (1.77 to 12.2 mmol g^{-1}) in terms of their textural and structural differences.

Keywords: activation; adsorption;zeolite; DTA; TG; XRF; XRD.

INTRODUCTION

Ammonia is a colorless, corrosive and pungent gas and is the most abundant alkaline component in the atmosphere. It is estimated that about 60 % of global ammonia emissions come from anthropogenic sources such as metabolic, agricultural and industrial processes. On the other hand, oceans, crops and biomass burning are also important.[1] Ammonia gas is irritating to throat, the skin, the eyes, nose and lungs. At high concentrations (1700 ppm) the gas causes extensive injuries and <30 min exposure may be fatal.[1,2] Studies related to experimental animals similarly show that exposure to high levels may adversely affect the respiratory system, the liver and spleen.[3] In addition, ammonia, one of the major environmental pollutants in water, is highly poisonous to fish and the toxicity is associated with the concentration of unionized ammonia (NH_3) which is dependent on the water pH value.[4]

* Corresponding author. E-mail: burcuerdogan@eskisehir.edu.tr
https://doi.org/10.2298/JSC211110051G

Available on line at www.shd.org.rs/JSCS/
(CC) 2022 SCS.

Atmospheric ammonia is a major aerial pollutant of poultry houses.[5] It has been reported that NH_3 concentrations are 5–20 ppm in the ventilation air of poultry and cattle houses and can reach up to 200 ppm during periods of low ventilation.[6] NH_3 should be removed from the environment as it can be hazardous to bird development and worker health.[7,8] There are many techniques such as catalytic decomposition and staged combustion processes in order to eliminate the ammonia emissions. In addition to these methods, NH_3 removal using natural zeolite is an alternative method due to its low cost, abundance and gas adsorption properties, which can be adjusted by cation exchange.

Zeolites are porous, crystalline, hydrated aluminosilicates containing alkali and alkaline earth cations. The zeolite framework has channels and interconnected voids and cavities occupied by the cations and water molecules.[9,10] Clinoptilolite is one of the most widely used natural zeolites. It contains three different channels. Channels A (10-membered ring, 0.44 nm×0.72 nm) and B (8-membered ring, 0.41 nm×0.47 nm) are parallel to each other and the c-axis, while the channels C (8-membered ring, 0.40 nm×0.55 nm) lies along *a*-axis, intersecting both channels A and B.[11] Within the clinoptilolite structure, Na^+ and Ca^{2+} are most efficient channel blockers and may occupy sites which are at the intersections of channels A/B with channel C, whilst the K^+ and Mg^{2+} have little effect on intersecting channels and reside in the centers of the C and A channels, respectively.[12–14] The high thermal and chemical stability and high internal surface area of this zeolite make it advantageous in removing hazardous gases.

Most of the studies on NH_3 removal have focused on 4A, 5A, 13X, faujasite, pentasil, ordered mesoporous carbon, activated alumina, alumina 1597, Cu-MOF-74, activated carbon and natural mordenite type materials.[15–22] Although studies on adsorption of ammonia by the natural clinoptilolite can be found in literature,[21,23–25] comparative studies on the effect of cation exchange and hydrochloric acid activation methods on thermal behavior and removal of ammonia gas by clinoptilolite have not been extensively performed. The novelty of this study is the detailed comparison of ammonia adsorption properties of both cation-exchanged and acid-modified forms of clinoptilolite type natural zeolite. Because the natural zeolites generally show low selectivity for NH_3, different methods should be used to increase this selectivity. The difference in the cation content of the mineral is one of the important factors that significantly affect the thermal properties of clinoptilolite and its affinity for polar gases, and thus its adsorption capacity. Therefore, the aim of this study is to examine natural and modified clinoptilolite samples in terms of chemical composition, thermal, structural and NH_3 adsorption properties.

EXPERIMENTAL

After grinding and sieving, the fraction below 63 μm of the natural clinoptilolite (CLN) from Gördes was used. The CLN label identifies a natural sample that has been free from any

(CC) 2022 SCS.

chemical treatment. Five grams of each zeolite were exchanged by refluxing with 100 mL of 1.0 M $Ca(NO_3)_2$, $Mg(NO_3)_2$, $NaNO_3$ and KNO_3 solutions at 90 °C for 5 h. Prepared zeolites were labeled as X-CLN, which the X indicate the type of exchanged cation. Acid activations were carried out using a 0.1 M and 1.0 M HCl solutions at the same experimental condition. The samples were named as 01H-CLN and 1H-CLN, respectively. Then, the suspensions were filtered, washed several times with de-ionized water at approximately boiling point and then the samples were dried in an oven at 110 °C for 20 h. The dried clinoptilolites were stored in a desiccator. All chemicals were supplied by Merck Company.

Chemical compositions were evaluated on powdered samples fused with lithium tetraborate using XRF analysis (Rigaku ZSX Primus instrument). Loss on ignition (*LOI*) was determined from the mass loss after heating samples to 1000 °C for 2 h. The crystal structure of the original and modified forms was determined by powder XRD technique using a D8 Advance Bruker instrument, with CuK_α radiation at 40 kV and 30 mA, in the range of 2θ values 5–40° and step range of 0.02° at room temperature. DTA and TG measurements were performed in the Setsys Evolution Setaram device at heating rate 10 °C min^{-1} in the temperature range of 30–1000 °C. In each run, *ca*. 35 mg of sample was loaded into the alumina pan. N_2 adsorption isotherm measured at 77 K using Autosorb 1, Quantachrome. Specific surface areas were determined by BET equation using the adsorption branch of the isotherms using the 0.05 to 0.35 P/P_0 range and the micropore data were calculated by applying the *t*-plot method. Ammonia adsorption isotherms of these zeolites were obtained at 298 K using the 3Flex-Micromeritics instrument. In each run, *ca*. 250 mg of clinoptilolite sample was loaded into the sample cell. The gases (N_2 and NH_3) used were highly pure (>99 %). Prior to gas adsorption measurements, all zeolite samples were degassed at 300 °C for 10 h.

RESULTS AND DISCUSSION

Chemical composition

The chemical compositions of the clinoptilolite samples are given in Table I. The water content of samples was estimated by the loss on ignition technique. Table I shows that the main cations found in CLN sample are potassium and calcium. In addition, iron is also present as an impurity. It was found that there was an increase in the amount of the exchangeable cations depending on the chosen salt solution compared to the raw sample, as expected.

TABLE I. Chemical composition of the clinoptilolite samples (wt. %)

Sample	Component							*LOI*
	SiO_2	Al_2O_3	Fe_2O_3	MgO	CaO	Na_2O	K_2O	%
CLN	70.823	12.850	1.249	0.619	2.241	0.561	5.171	6.332
Na-CLN	71.178	12.809	1.178	0.383	0.471	3.490	3.686	6.430
K-CLN	70.465	12.740	1.118	0.393	0.176	0.185	9.855	5.078
01H-CLN	73.501	12.138	1.375	0.560	1.466	–	4.770	6.192
1H-CLN	81.284	8.219	1.175	0.351	0.378	–	2.314	6.150
Ca-CLN	70.836	12.631	1.271	0.506	3.762	–	3.316	7.595
Mg-CLN	70.641	12.641	1.285	2.012	1.433	0.281	3.638	8.070

After the clinoptilolite activated with hydrochloric acid solutions, aluminum and the exchangeable cations were removed from the material. On the other

(CC) 2022 SCS.

hand, it was determined that the SiO_2 content increased with increasing acid molarity due to its insolubility. SiO_2/Al_2O_3 ratio for CLN sample increased from 5.5 to 6.0 and 9.9 in the 01H-CLN and 1H-CLN, respectively, indicating the gradual removal of aluminum from the structure (Table I).

X-Ray analysis

Powder XRD patterns of all the clinoptilolite samples are shown in Fig. 1. In addition to the main clinoptilolite (characteristic peaks at 2θ 9.83, 15.90, 22.4 and 30°) phase, minor amounts of illite, feldspar and opal CT were also identified.

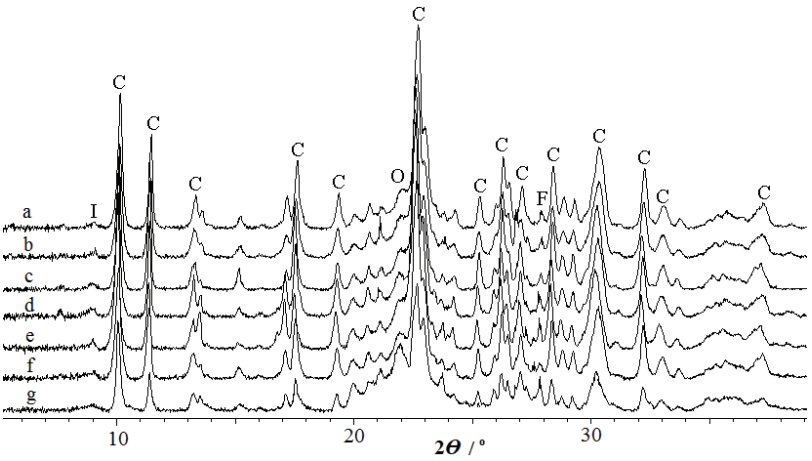

Fig. 1. X-ray powder diffraction patterns of the CLN (a), Na-CLN (b), K-CLN (c), Ca-CLN (d), Mg-CLN (e), 01H-CLN (f) and 1H-CLN (g) samples (C: clinoptilolite, I: illite, O: opal-CT, F: feldspar).

The quantitative XRD analysis demonstrated that the major component of the natural sample (CLN) is clinoptilolite (80 %), with minor amounts of opal A (4–5 %), opal-CT (4–5 %), smectite (1–2 %), mica-illite (1–2 %) and feldspar (6–7 %). The method given by Esenli and Sirkecioğlu[26] was used to determine the mineral ratio. It was determined that there was no significant change in the intensity of major clinoptilolite peaks in the clinoptilolite samples modified with different salt solutions. As a result of the dealumination (Table I) and partial destruction of the crystal structure, the intensity of the main clinoptilolite peaks for 1H-CLN decreased gradually. In addition, as the acid concentration increased, the crystallinity of the sample decreased and there is a broad hump in between 20–30° (2θ) on the patterns of the acid activated samples (Fig. 1g). Similar changes were obtained in previous studies on the activation of clinoptilolite with acid solutions.[27,28]

(CC) 2022 SCS.

Nitrogen adsorption

N_2 adsorption isotherms of the samples are presented in Figs. 2 and 3 (relative pressure P/P_0 *vs*. adsorbed volume in cm^3 STP per g of clinoptilolite). All clinoptilolite samples show type-II isotherms.[29] The values of the specific surface areas and, micropore data of the samples are presented in Table II. It was determined that the specific surface areas of cation exchanged clinoptilolite samples increased slightly. Whilst it was found that 1.0 M HCl treatment (203 m^2 g^{-1}) caused about 5 times increase in specific surface area of CLN (42 m^2 g^{-1}). This result agrees well with the X-ray diffraction data (Fig. 1). As seen from Table I, the increase in the micropore areas and micropore volumes for acid activated (01H-CLN and 1H-CLN) samples is obviously due to the unblocking of the channels of the clinoptilolite through decationation and dealumination and the formation of secondary porosity owing to the dissolution of the free linkages.

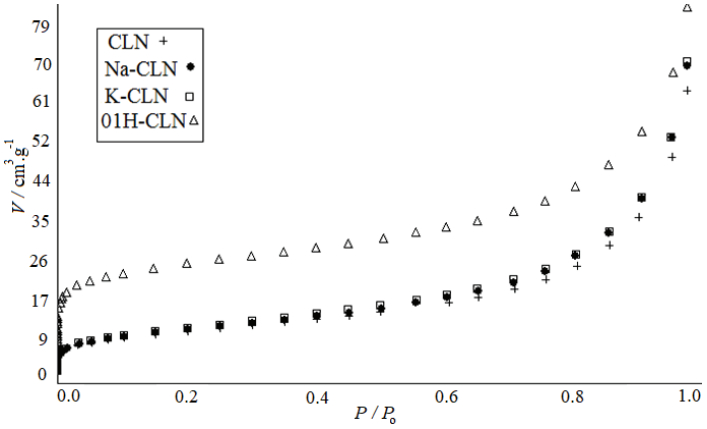

Fig. 2. Nitrogen adsorption isotherms of CLN, Na-CLN, K-CLN and 01H-CLN samples.

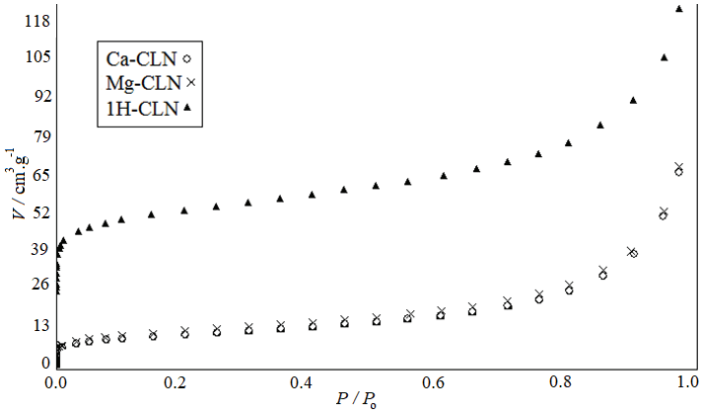

Fig. 3. Nitrogen adsorption isotherms of Ca-CLN, Mg-CLN and 1H-CLN samples.

(CC) 2022 SCS.

TABLE II. Nitrogen adsorption data of the natural and modified clinoptilolite samples

Sample	Surface area, $m^2 g^{-1}$		Volume, $cm^3 g^{-1}$	
	BET	Micropore	Micropore	Total pore
CLN	42	10.0	0.004	0.100
Na-CLN	43	8.5	0.003	0.109
K-CLN	44	6.5	0.003	0.110
01H-CLN	97	54.6	0.023	0.129
1H-CLN	203	135.1	0.056	0.193
Ca-CLN	44	12.1	0.005	0.105
Mg-CLN	48	11.5	0.006	0.109

Thermal analysis (TG-DTA)

The DTA and TG curves of the clinoptilolite samples over the temperature range 30–1000 °C are shown in Fig. 4. DTA curves of clinoptilolite samples

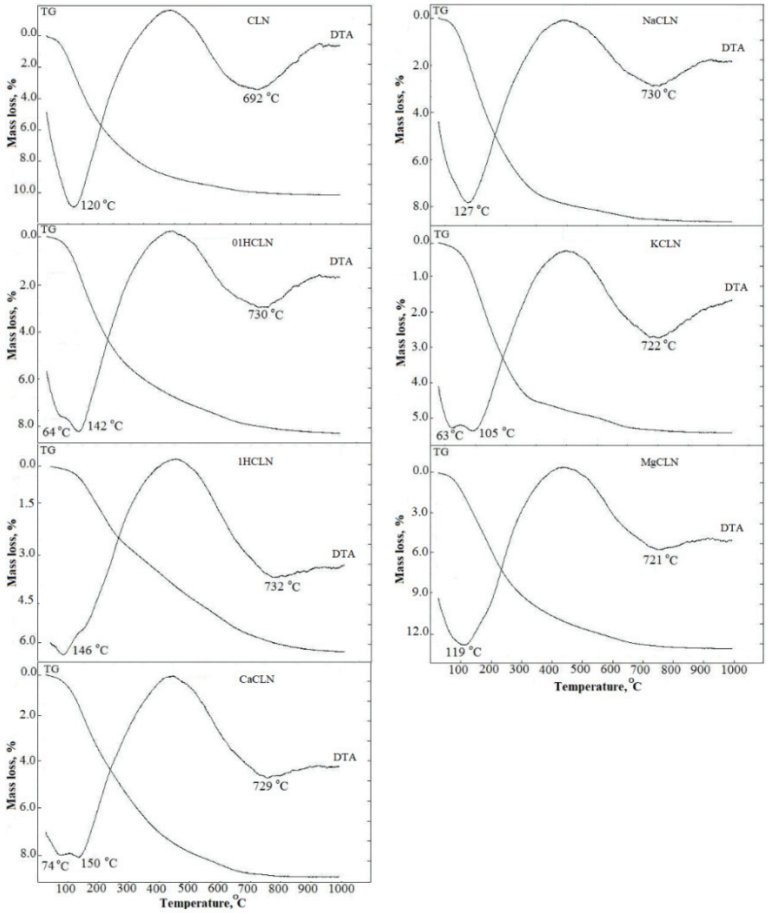

Fig. 4. TG-DTA curves of all clinoptilolite samples.

(CC) 2022 SCS.

show the endotherms at temperature ranging from 63–74 °C and 120–150 °C between 30 and 200 °C as a result of the dehydration process. Third endothermic peaks at 692 to 732 °C in the temperature interval from 600 to 800 °C are due to the dehydroxylation. TG curves display the major mass losses (1.61 to 5.55 %) owing to the loss of the water located in the cavities and bound to the nonframework cations. In the temperature range between 200 and 600 °C more strongly associated water (2.79 to 6.46 %) is eliminated. In the temperature range from 600 to 800 °C, the rest of the water (0.28 to 0.70 %) is gradually removed. As seen in Fig. 4, clinoptilolite samples showed continuous mass loss curves and the mass losses are constant at temperatures above 800 °C.

For the cation exchanged samples, the mass losses recorded by TG analysis increased in the order of K-CLN < Na-CLN < Ca-CLN < Mg-CLN (Table III). The thermal behaviour of the clinoptilolite depends on many parameters such as the type of the exchangeable cations, their coordination to water molecules and their hydration energies.[30] It was found that the mass loss values were higher in clinoptilolites exchanged with divalent cations (Mg^{2+} and Ca^{2+}) with the high-hydration energies than those of exchanged with monovalent cations (K^+ and Na^+) with low-hydration energies. Moreover, for monovalent and divalent cations, less zeolite water loss of samples exchanged with larger sized cations can be attributed to the smaller space remaining in the zeolite structure.

TABLE III. Mass loss (%) of the natural and modified clinoptilolite samples at different temperature ranges

Sample	Temperature range, °C					Total
	30–200	200–400	400–600	600–800	800–1000	
CLN	5.50	3.23	0.92	0.42	0.09	10.17
Na-CLN	4.66	3.22	0.58	0.31	0.05	8.82
K-CLN	2.53	2.29	0.50	0.28	0.03	5.63
01H-CLN	3.64	2.75	1.08	0.54	0.13	8.14
1H-CLN	1.61	2.11	1.50	0.85	0.21	6.28
Ca-CLN	4.66	3.22	0.59	0.31	0.05	8.83
Mg-CLN	5.55	4.85	1.61	0.70	0.11	12.82

In the case of acid activated forms, the mass losses for the acid-treated clinoptilolites (6.28 and 8.14 %) are lower than that for the CLN (10.17 %). This can be explained by the elimination of the exchangeable cations and the dealumination (Table I).

Adsorption of NH_3

The ammonia adsorption isotherms of the raw, cation exchanged and acid activated variants were measured at 298 K (Figs. 5 and 6). All the isotherms are of type I.[29] The adsorption rate of ammonia on all samples decreased in the

(CC) 2022 SCS.

order: Mg-CLN > Ca-CLN > Na-CLN > 01H-CLN > CLN > 1H-CLN > K-CLN (Table IV).

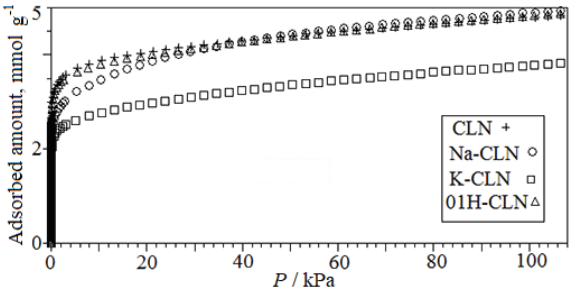

Fig. 5. Ammonia adsorption isotherms of CLN, Na-CLN, K-CLN and 01H-CLN samples at 298 K.

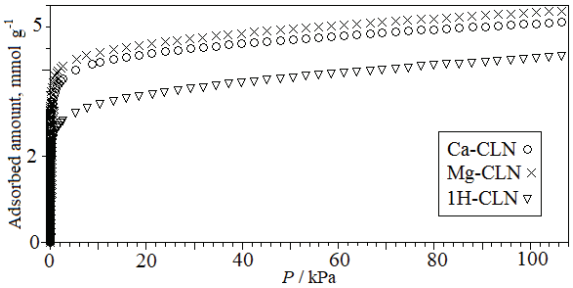

Fig. 6. Ammonia adsorption isotherms of Ca-CLN, Mg-CLN and 1H-CLN samples at 298 K.

TABLE IV. Ammonia uptake for various materials

Sample	Temperature, K	Adsorption capacity, mmol g^{-1}	Reference
CLN	298	4.840	Present work
Na-CLN	298	4.947	Present work
K-CLN	298	3.823	Present work
01H-CLN	298	4.875	Present work
1H-CLN	298	4.312	Present work
Ca-CLN	298	5.159	Present work
Mg-CLN	298	5.372	Present work
Alumina 1597	298	3.008	15
Silica gel 40	298	6.250	15
Clinoptilolite	298	5.904	15
13X	298	9.326	15
Pentasil dealuminated	298	2.34	15
Faujasite dealuminated	298	1.77	15
Activated carbon	298	4.19	15
Zs	295	6.30 mg g^{-1}	23
Mesoporous carbon	298	6.39	17
Activated alumina	298	2.53	18

(CC) 2022 SCS.

TABLE IV. Continued

Sample	Temperature, K	Adsorption capacity, mmol g^{-1}	Reference
Natural clinoptilolite from Nizny Hrabovec	298	0.705	25
Natural clinoptilolite from Nizny Hrabovec	293	0.634	33
Natural clinoptilolite from Nizny Hrabovec	293	1.268	33
Natural clinoptilolite from Nizny Hrabovec treated with 30 % H_2SO_4	293	1.174	33
Natural clinoptilolite from Nizny Hrabovec treated with 30 % H_3PO_4	293	1.121	33
Natural clinoptilolite from Nizny Hrabovec treated with 30 % HNO_3	293	1.121	33
Cu-MOF-74	298	3.4	32
4A zeolite	298	8.71	15
In-PMOF	298	9.41	31
MOF-177	298	12.2	19

Due to the fact that the kinetic diameter of the ammonia molecule is 0.26 nm, it can penetrate into the zeolite channels of clinoptilolite. As can be seen from Figs. 5 and 6, the maximal sorption capacity of ammonia is exhibited by Mg-CLN sample (5.372 mmol g^{-1}) and minimal by K-CLN (3.823 mmol g^{-1}). Obviously, the gas adsorption on zeolites depends on many parameters such as their structure, size and distribution of the exchangeable cations within their channels, and features of the adsorbate (size, geometry and polarity, etc.). Na^+ and Ca^{2+} located at the intersections of the A/B channels with the C channel in the clinoptilolite structure are the most effective channel blockers, while the K^+ and Mg^{2+} cations have little effect on intersecting channels and they are located in the centers of the C and A channels, respectively.[12–14]

Hence, limited access to channels and consequent lower ammonia uptake of Na-CLN and Ca-CLN samples compared to Mg-CLN sample are due to the increased amount of Na^+ and Ca^{2+} in the channel A and B, respectively and continued presence of K^+ (Table I). In the Mg-CLN sample with the highest ammonia adsorption capacity, the location of this small cation in channel A caused more space between channels and increased NH_3 gas uptake. The lowest ammonia adsorption capacity for K-CLN can be attributed to its size (largest) and the location of the K^+ in the channel C. For this reason, it appears that the location of the exchangeable cations has a greater influence on adsorption capacity than the amount or size of the cations.

The wide variation in the adsorption capacity of ammonia gas for the cation exchanged clinoptilolites indicates that both electrostatic forces and dispersion forces played an active role in the adsorption dynamics of the adsorbents studied.

(CC) 2022 SCS.

In addition, the high affinity for NH_3 can be attributed to the specific interactions of the permanent dipole moment (1.47 D*) of NH_3 molecule with the electric field created by the cations in the zeolite structure. 01-HCLN sample (4.875 mmol g^{-1}) exhibited a lower adsorption capacity than the Mg-CLN sample due to the removal of the cations from the structure and thus a decrease in the local electric field. Although 1H-CLN had the highest specific surface area (203 m^2 g^{-1}), its NH_3 uptake (4.312 mmol g^{-1}) was lower than those of CLN (4.840 mmol g^{-1}) and 01-HCLN (4.875 mmol g^{-1}) owing to the partial destruction of the crystal structure as presented by XRD data (Fig. 1) and XRF analysis (Table I).

When the ammonia adsorption capacities of all samples were compared, the adsorption capacity of raw clinoptilolite (CLN) was somewhere in between. This can be attributed to the mixed cationic (*i.e.*, Na^+, K^+ and Ca^{2+}) content of the CLN sample and partial blockages in the channel structure that allow less passage of the NH_3 molecule through the channels. CLN sample (4.840 mmol g^{-1}) adsorbed less ammonia gas than clinoptilolite from Mud Hills, USA (5.904 mmol g^{-1})[15] due to its different origin and mineral content. As seen from Table IV, retention of ammonia gas by Mg-CLN sample (5.372 mmol g^{-1}) were smaller than MOF-177 (12.2 mmol g^{-1}),[19] In-PMOF (9.41 mmol g^{-1}),[31] silica gel 40 (6.250 mmol g^{-1}),[15] 13X (9.326 mmol g^{-1}),[15] mesoporous carbon (6.39 mmol g^{-1})[17], 4A zeolite (8.71 mmol g^{-1})[15] but were higher than those of alumina 1597 (3.008 mmol g^{-1}),[15] faujasite dealuminated (1.77 mmol g^{-1})[15], pentasil dealuminated (2.34 mmol g^{-1}),[15] activated carbon (4.19 mmol g^{-1}),[15] Cu-MOF-74 (3.4 mmol g^{-1})[32] and natural clinoptilolite (from Nizny, Hrabovec) treated with 30 % H_2SO_4 (1.268 mmol g^{-1})[33]. It should be noted here that the structural and textural properties of all these synthetic materials are different from the sample of the present article. Although natural zeolites contain high levels of major mineral components, they often contain impurities in their structure. In addition, due to their uniform and tunable nature, synthetic zeolites generally show higher gas adsorption capacities than natural zeolites, but have the disadvantage of being more expensive than natural ones.

The abundance and high sorption capacity of the clinoptilolite-type natural zeolite provide low-cost and eco-friendly solutions. For this reason, the Mg-CLN sample with the highest capacity can be proposed as an effective adsorbent in environments where ammonia gas needs to be removed, such as poultry houses.

CONCLUSION

Our paper presents a novel view of discussion on the effect of cation content on the thermal and ammonia adsorption properties of clinoptilolite-rich tuff. The following conclusions can be drawn from the obtained results of this study.

* 1 D = 3.34×10^{-30} C m

(CC) 2022 SCS.

1. XRF data show that significant changes occurred in the cation content of the clinoptilolite following both cation exchange and acid treatment. In addition, the thermal behavior of the clinoptilolite was affected by the dominant cation in the structure.

2. The powder XRD analysis demonstrated that treatment of clinoptilolite with 1.0 M HCl solutions at 90 °C for 5 h caused a partial destruction in structure and a significant decrease in ammonia adsorption capacity.

3. When using different cations for modification, the amount, size and location of the exchangeable cations in the zeolite structure were found to be more efficient than the extent of exchange in NH_3 adsorption. For the cation exchanged clinoptilolites, ammonia adsorption capacity decreased with the increasing cation radii.

4. Our study shows that Mg-CLN material exhibited the maximal ammonia adsorption capacity among all the clinoptilolite samples and thus this sample might be a good candidate for removing ammonia pollution from the environment.

Acknowledgements. This research was supported by the Anadolu University Commission of Scientific Research Project No. 1602F072. Special thanks to Prof. Dr. Matthias Thommes for his valuable insights and recommendations.

ИЗВОД

УКЛАЊАЊЕ NH_3 ПРИРОДНИМ И МОДИФИКОВАНИМ КЛИНОПТИЛОЛИТОМ

AYTAÇ GÜNAL[1] и BURCU ERDOĞAN[2]

[1]*Eskisehir Technical University, Graduate School of Sciences, Yunusemre Campus, 26470 Tepebasi, Eskisehir, Turkey и* [2]*Eskisehir Technical University, Faculty of Science, Department of Physics, Yunusemre Campus, 26470 Tepebasi, Eskisehir, Turkey*

Процеси катјонске измене и киселинске активације су коришћени да би се испитали ефекти различитих катјона у саставу клиноптилолита на адсорпцију амонијака. Термогравиметрија (TG), диференцијална термијска анализа (DTA), дифракција X-зрачења (XRD), флуоресценција X-зрачења (XRF) и адсорпција азота су технике коришћене за карактеризацију узорака клиноптилолита. Као резултат јонске измене и киселинске активације, количина, тип и положај измењених катјона у структури је значајно утицао на термалне особине као и на ефикасност уклањања NH_3. Адсорпционе изотерме за амонијак су добијене на 298 K и до 100 kPa волуметријски. Додатно, адсорпциони капацитети узорака клиноптилолита за NH_3 (3,823–5,372 mmol g^{-1}) су упоређени са адсорпционим капацитетима других материјала (1,77–12,2 mmol g^{-1}) ради утврђивања њихових текстуралних и стуктурних разлика.

(Примљено 10. новембра 2021, ревидирано 30. маја, прихваћено 11. јуна 2022)

REFERENCES

1. P. Carson, C. Mumford, *Hazardous Chemicals Handbook*. Butterworth-Heinemann, Oxford, 2002, pp. 276–279 (https://www.elsevier.com/books/hazardous-chemicals handbook/carson/978-0-7506-4888-2)

(CC) 2022 SCS.

2. N. I. Sax, *Dangerous Properties of Industrial Materials*, Van Nostrand Reinhold, New York, 1984, p. 1251 (https://aiche.onlinelibrary.wiley.com/doi/abs/10.1002/aic.690260134)
3. *Toxicological Review of Ammonia Noncancer Inhalation: Executive Summary*, 2020 (https://cfpub.epa.gov/ncea/iris/iris_documents/documents/subst/0422_summary.pdf, Accessed 26 August 2021)
4. F. B. Eddy, in *Water/Air Transitions in Biology*, A. K. Mittal, F. B. Eddy, J. S. Datta Munshi, Eds., Science Publishers Inc, Enfield, NH, 1999, p. 281 (https://www.amazon.com/Water-Air-Transition-Biology-Mittal/dp/1578080592)
5. H. H. Kristensen, C. Wathes, *Worlds Poult. Sci. J.* **56** (2000) 235 (https://doi.org/10.1079/WPS20000018)
6. E. F. Wheeler, K. D. Casey, R. S. Gates, H. Xin, J. L. Zajaczkowski, P. A. Topper, Y. Liang, A. J. Pescatore, *Trans. ASABE* **49** (2006) 1495 (https://doi.org/10.13031/2013.22042)
7. D. M. Miles, S. L. Branton, B. D. Lott, *Poultry Sci.* **83** (2004) 1650 (https://doi.org/10.1093/ps/83.10.1650)
8. K. J. Donham, D. Cumro, S. Reynolds, *J. Agromed.* **8** (2002) 57 (https://doi.org/10.1300/J096v08n02_09)
9. D. W. Breck, *Zeolite Molecular Sieves*, Wiley, New York 1984 (https://books.google.com.tr/books/about/Zeolite_Molecular_Sieves.html?id=aY0vAQAAIAAJ&redir_esc=y)
10. G. Gottardi, E. Galli, *Natural zeolites*, Springer, Berlin, 1985 (https://link.springer.com/book/10.1007/978-3-642-46518-5)
11. M. W. Ackley, R. F. Giese, R. T. Yang, *Zeolites* **12** (1992) 780 (https://doi.org/10.1016/0144-2449(92)90050-Y)
12. K. Koyama, Y. Takeuchi, *Z. Krist.* **145** (1977) 216 (https://doi.org/10.1524/zkri.1977.145.3-4.216)
13. T. Armbruster, M. E. Gunter, in *Reviews in Mineralogy and Geochemistry, Natural Zeolites: Occurrences, Properties, Applications*, D. L. Bish, D. W. Ming, Eds. Mineralogical Society of America, Washington DC, 2001, p. 1 (https://pubs.geoscienceworld.org/msa/rimg/article-abstract/45/1/1/140719/Crystal-Structures-of-Natural-Zeolites?redirectedFrom=fulltext)
14. E. Kouvelos, K. Kesore, T. Steriotis, H. Grigoropoulou, D. Bouloubasi, N. Theophilou, S. Tzintzos, N. Kanelopoulos, *Micropor. Mesopor. Mater.* **99** (2007) 106 (https://doi.org/10.1016/j.micromeso.2006.07.036)
15. J. Helminen, J. Helenius, E. Paatero, I. Turunen, *J. Chem. Eng. Data* **46** (2001) 391 (https://doi.org/10.1021/je000273+)
16. L. Benco, D. Tunega, *Phys. Chem. Miner.* **36** (2009) 281 (https://doi.org/10.1007/s00269-008-0276-9)
17. D. Saha, S. Deng, *J. Colloid Interface Sci.* **345** (2010) 402 (https://doi.org/10.1016/j.jcis.2010.01.076)
18. D. Saha, S. Deng, *J. Chem. Eng. Data* **55** (2010) 5587 (https://doi.org/10.1021/je100405k)
19. D. Saha, S. Deng, *J. Colloid Interface Sci.* **348** (2010) 615 (https://doi.org/10.1016/j.jcis.2010.04.078)

(CC) 2022 SCS.

20. D.T. Hayhurst, *Chem. Eng. Commun.* **4** (1980) 729 (https://doi.org/10.1080/0098644-8008935944)
21. D. Kallo, J. Papp, J. Valyon, *Zeolites* **2** (1982) 13 (https://doi.org/10.1016/S0144-2449(82)80034-1)
22. C. C. Huang, H. S. Li, C. H. Chen, *J. Hazar. Mater*. **159** (2008) 523 (https://doi.org/10.1016/j.jhazmat.2008.02.051)
23. H. Asilian, S. B. Mortazav, H. Kazemian, S. Phaghihzadeh, Sj. Shahtaheri, M. Salem, *Iran J. Public Health* **33** (2004) 45 (https://ijph.tums.ac.ir/index.php/ijph/article/view/1929)
24. D. Caputo, B. De Gennaro, B. Liguori, M. Pansini, C. Colella, *Stud. Surf. Sci. Catal*. **140** (2001) 121 (https://doi.org/10.1016/S0167-2991(01)80142-7)
25. K. Ciahotny, L. Melenova, H. Jirglova, O. Pachtova, M. Kocirık, M. Eic, *Adsorption* **12** (2006) 219 (https:// doi.org/ 10.1007/s10450-006-0148-x)
26. F. Esenli, A. Sirkecioğlu, *Clay Miner.* **40** (2005) 557 (https://doi.org/10.1180/0009855054040192)
27. G. E. Christidis, D. Moraeti, E. Keheyan, L. Akhalbedashvili, N. Kekelidze, R. Gevorkyan, H. Yeritsyan, H. Sargsyan, *Appl. Clay Sci*. **24** (2003) 79 (https://doi.org/10.1016/S0169-1317(03)00150-9)
28. Radosavljević-Mihajlović, V. Dondur, A. Daković, J. Lemic, M. Tomašević-Čanović, *J. Serb. Chem. Soc.* **69** (2004) 273 (https://doi.org/10.2298/JSC0404273R)
29. S. Lowell, J.E. Shields, M.A. Thomas, M. Thommes, *Characterization of porous solids and powders: surface area, pore size and density*, Springer, Amsterdam, 2006 (https://link.springer.com/book/10.1007/978-1-4020-2303-3)
30. D. L. Bish, in *Occurrence, properties and utilization of natural zeolites*, D. Kallo, H. S. Sherry, Eds., Akademiai Kiado, Budapest, 1988, p. 565 (https://books.google.com.tr/books/about/Occurrence_Properties_and_Utilization_of.html?id=e1LwAAAAMAAJ&redir_esc=y)
31. S. Moribe, Z. Chen, S. Alayoglu, Z. H. Syed, T. Islamoglu, O. K. Farha, *ACS Mater. Lett.* **1** (2019) 476 (https://doi.org/10.1021/acsmaterialslett.9b00307)
32. M. J. Katz, A.J. Howarth, P.Z. Moghadam, J.B. DeCoste, R.Q. Snurr, J. T. Hupp, O. K. Farha, *Dalton Trans.* **45** (2016) 4150 (https://doi.org/10.1039/C5DT03436A)
33. K. Ciahotny, L. Melenova, H. Jirglova, M. Boldis, M. Kocirik, in *Studies in Surface Science and Catalysis,* Vol. 142, R. Aiello, G. Giordano, F. Testa, Eds., Elsevier Science, Amsterdam, 2002, p. 1713 (https://doi.org/10.1016/S0167-2991(02)80344-5).

(CC) 2022 SCS.